Design, Synthesis, Structural Studies, Biological Evaluation, and Computational Simulations of Novel Potent AT_1 Angiotensin II Receptor Antagonists Based on the 4-Phenylquinoline Structure

Andrea Cappelli,*[,‡] Gal.la Pericot Mohr,[‡] Andrea Gallelli,[‡] Milena Rizzo,[▽] Maurizio Anzini,[‡] Salvatore Vomero,[‡] Laura Mennuni,[§] Flora Ferrari,[§] Francesco Makovec,[§] M. Cristina Menziani,[†] Pier G. De Benedetti,[†] and Gianluca Giorgi[||]

Dipartimento Farmaco Chimico Tecnologico and European Research Centre for Drug Discovery and Development, Università di Siena, Via A. Moro, 53100 Siena, Italy, Dipartimento di Scienze Farmacobiologiche, Università "Magna Græcia" di Catanzaro, Complesso "Ninì Barbieri", 88021 Roccelletta di Borgia, Catanzaro, Italy, Rotta Research Laboratorium S.p.A., Via Valosa di Sopra 7, 20052 Monza, Italy, Dipartimento di Chimica, Università degli Studi di Modena e Reggio Emilia, Via Campi 183, 41100 Modena, Italy, and Centro Interdipartimentale di Analisi e Determinazioni Strutturali, Università di Siena, Via A. Moro, 53100 Siena, Italy

Received November 6, 2003

Novel AT_1 receptor antagonists bearing substituted 4-phenylquinoline moieties instead of the classical biphenyl fragment were designed and synthesized as the first step of an investigation devoted to the development of new antihypertensive agents and to the understanding of the molecular basis of their pharmacodynamic and pharmacokinetic properties. The newly synthesized compounds were tested for their potential ability to displace [^{125}I]Sar^1,Ile^8-Ang II specifically bound to AT_1 receptor in rat hepatic membranes. These AT_1 receptor binding studies revealed nanomolar affinity in several of the compounds under study. The most potent ligands **4b**,**t** were found to be equipotent with losartan and possessed either a 3-tetrazolylquinoline or a 2-amino-3-quinolinecarboxylic moiety, respectively. Moreover, some selected compounds were evaluated for antagonism of Ang II-induced contraction in rabbit aortic strips, and the most potent compounds in the binding test **4b**,**t** were slightly more potent than losartan in inhibiting Ang II-induced contraction. Finally, the most relevant structure-affinity relationship data were rationalized by means of computational studies performed on the isolated ligands as well as by computational simulations on the ligands complexed with a theoretical AT_1 receptor model.

Introduction

Angiotensin II (Ang II) is an octapeptide produced by the renin−angiotensin system (RAS), which plays a key role in the pathophysiology of hypertension. This vasoactive hormone regulates the cardiovascular homeostasis by acting on both the vascular resistance and the blood volume. Ang II is produced in vivo from angiotensin I by the angiotensin converting enzyme (ACE).[1] ACE inhibitors such as Enalapril and Captopril are largely used in clinic in the treatment of hypertension, and the commercial success of these drugs demonstrates the modulation of RAS to represent a very interesting approach to the control of hypertension. However, ACE is not a very selective enzyme, as it possess among its substrates important peptides such as bradykinin and substance P. In fact, the pharmacological properties of ACE inhibitors, but also some of the major side effects associated with their clinical use (such as dry cough, angioedema, and rashes), may be related to bradykinin potentiation.[2] Thus, the specific block of Ang II actions at the receptor level represents a potentially convenient approach to modulate the RAS. In humans, two main Ang II receptor subtypes have been characterized and called AT_1 and AT_2.[1,3]

The AT_1 receptor subtype mediated virtually all the known physiological actions of Ang II in cardiovascular, neuronal, endocrine, hepatic, and in other cells. This receptor belongs to the G protein-coupled receptor (GPCR) superfamily and shows the seven hydrophobic transmembrane domains forming α-helices in the lipid bilayer of the cell membrane. The interaction of Ang II with AT_1 receptor induces a conformational change, which promotes the coupling with the G protein(s) and leads to the signal transduction via several effector systems (phospholipases C, D, A_2, adenyl cyclase, etc.).[1,4]

The parallel discovery of losartan and eprosartan, potent and orally active nonpeptide Ang II antagonists, has stimulated the design of a large number of congeners.[5] Among them, irbesartan, candesartan, valsartan, telmisartan, and olmesartan are on the market and about 20 other compounds are being developed. Most of these compounds have the biphenyl fragment bearing an acidic moiety (tetrazole ring, COOH, SO_2NHCO) in common and differ in the nature of the pendent heterocyclic system (valsartan lacks the heterocyclic moiety) connected to the para position of the distal phenyl by means of a methylene group. In fact, in the design of new nonpeptide Ang II antagonists, the strategy followed by most medicinal chemists concerned the molecular modification of the imidazole moiety of losartan (**1**) (Chart 1). Among the large variety of the heterocyclic

* To whom correspondence should be addressed. Tel: +39 577 234320. Fax: +39 577 234333. E-mail: cappelli@unisi.it.

[‡] Dipartimento Farmaco Chimico Tecnologico European Research Centre for Drug Discovery and Development, Università degli Studi di Siena.

[▽] Dipartimento di Scienze Farmacobiologiche, Università "Magna Græcia" di Catanzaro.

[§] Rotta Research Laboratorium S.p.A.

[†] Dipartimento di Chimica, Università degli Studi di Modena e Reggio Emilia.

[||] Centro Interdipartimentale di Analisi e Determinazioni Strutturali, Università di Siena.

10.1021/jm031100t CCC: $27.50
Published on Web 04/10/2004

Chart 1

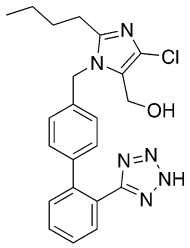

losartan (**1**)

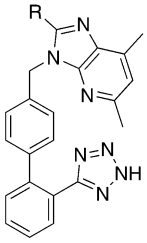

2a (R = C_2H_5, L-158,809)
2b (R = *n*-C_3H_7)

Chart 2

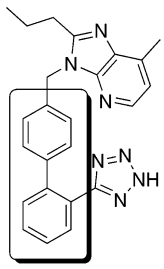

2c (L-158,338)
IC_{50} = 1 nM

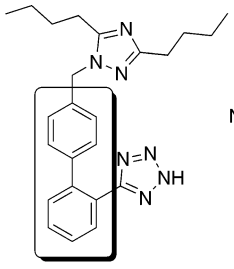

3a (SC-50560)
IC_{50} = 5.6 nM

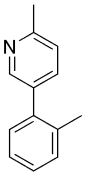

3b
6.8 nM

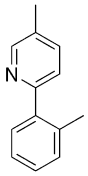

3c
6.9 nM

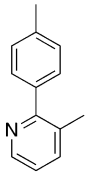

2d
116 nM

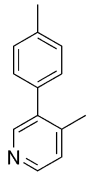

2e
not available

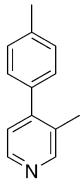

2f
4 nM

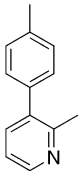

2g
60 nM

3d
98 nM

3e
150 nM

3f
250 nM

3g
110 nM

systems developed, an outstanding position is occupied by the imidazo[4,5-*b*]pyridine moiety of compound **2a** (L-158,809).[6] This congener of losartan has been reported to show a subnanomolar AT_1 receptor affinity about 2 orders of magnitude higher than that of losartan and represents one of the most potent nonpeptide Ang II antagonists developed. This suggests that the stereoelectronic characteristics of the imidazo[4,5-*b*]pyridine moiety can be considered optimal for the interaction with the receptor. On the other hand, relatively little information is available on the effects of the molecular modification of the phenyl group bearing the acidic moiety (distal phenyl ring). While the design was being performed, our attention was captured by the report that the introduction of a nitrogen atom in the distal phenyl of compound **3a** (SC-50560) had detrimental effects on the AT_1 receptor affinity independent of the position occupied by the nitrogen atom (see Chart 2), while negligible effects were seen when this kind of modification involved the proximal phenyl group.[7] On the other hand, similar molecular modifications performed on imidazo[4,5-*b*]pyridine derivative **2c** (L-158,338) gave slightly different results.[8] For example, the introduction of the nitrogen atom in para-position (with respect to the proximal phenyl ring) of **3a** distal phenyl led to a 45-fold affinity decrease, while the same modification performed on imidazo[4,5-*b*]pyridine derivative **2c** had less dramatic effects (only a 4-fold loss in AT_1 binding affinity). Moreover, 4-phenyl-3-tetrazolylpyridyl derivative **2f** was reported to be an orally active Ang II antagonist showing a somewhat poorer oral bioavailability than **2c**. The authors suggested that the decrease in the lipophilicity had a negative effect on the oral potency of compound **2f** with respect to **2c**.[8]

Chart 3

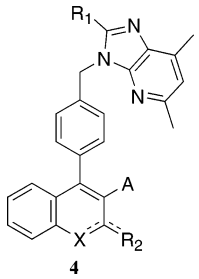

4

Scheme 1[a]

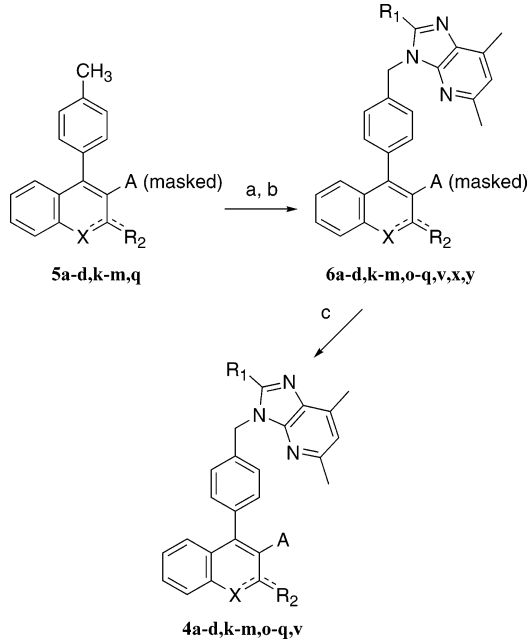

[a] Reagents: (a) NBS, dibenzoyl peroxide, CCl_4; (b) 2-substituted-5,7-dimethyl-3*H*-imidazo[4,5-*b*]pyridine, NaH, DMF; (c) HCOOH (for tetrazole derivatives **4b**,**l**,**o**) or NaOH (for carboxylates **4a**,**c**,**d**,**k**,**m**,**p**,**q**,**v**).

Taken together, these observations revealed the complex nature of the ligand−receptor interaction stimulating the design of some molecular modifications involving distal phenyl group of compounds **2** which led to the development of compounds **4** (Chart 3). In this paper we describe the synthesis, the structural and the pharmacological characterization, the structure−affinity relationships (SAFIR), and the ligand−receptor interaction simulations of the novel Ang II antagonists **4** as the first step of an investigation devoted to both the development of new antihypertensive agents and the understanding of the molecular basis of their pharmacodynamic and pharmacokinetic[9] properties.

Chemistry

The preparations of the target compounds **4a**−**d**, **k**−**m**,**o**−**q**,**v** were carried out in three steps starting from the suitable toluene derivatives by benzylic bromination, coupling reaction with substituted imidazo-[4,5-*b*]pyridines,[6,10] and unmasking of the acidic (carboxylic or tetrazole) moiety (Scheme 1).

Scheme 2[a]

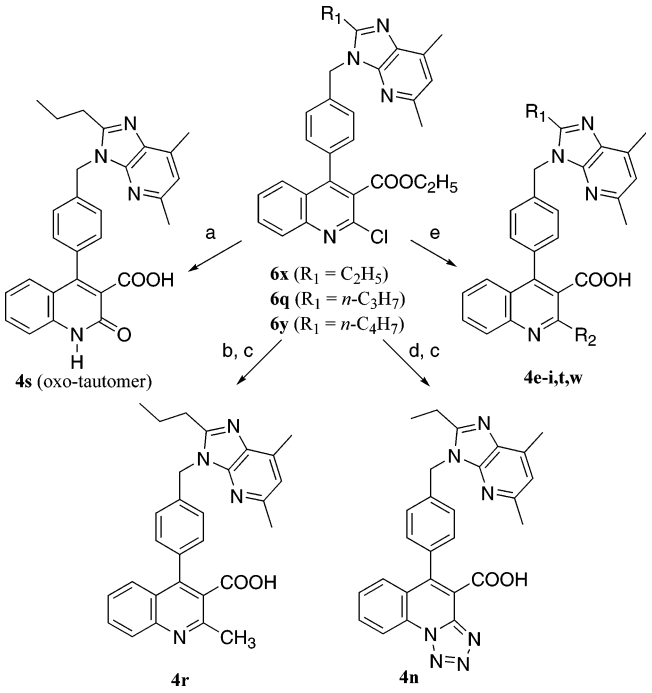

[a] Reagents: (a) NaOH, dioxane; (b) $(CH_3)_4Sn$, $Pd(PPh_3)_2Cl_2$, DMF; (c) NaOH, C_2H_5OH; (d) NaN_3, DMF; (e) (**4e**,**t**,**w**, R_2 = NH_2): $C_2H_5OCOCH_2NH_2HCl$, C_5H_5N, then NaOH, C_2H_5OH; (**4f**,**h**, R_2 = NHR): RNH_2, C_2H_5OH, then NaOH, C_2H_5OH; (**4g**,**i**, R_2 = NRR): RRNH, C_2H_5OH (or DMF), then NaOH, $HOCH_2CH_2OH$.

Scheme 3[a]

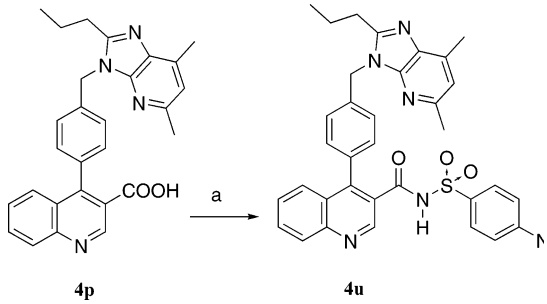

[a] Reagents: (a) EDCI, DMAP, *p*-$NO_2C_6H_4SO_2NH_2$, CH_2Cl_2.

Scheme 4[a]

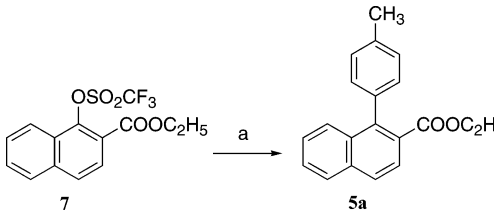

[a] Reagents: (a) *p*-$CH_3C_6H_4B(OH)_2$, Na_2CO_3, LiCl, Pd/C, DMF.

Other target 3-quinolinecarboxylic acids showing different substituents in position 2 of the quinoline nucleus (compounds **4e**−**i**,**r**−**t**,**w**) were synthesized by means of the suitable elaboration of the intermediate iminochlorides **6q**,**x**,**y**. The chlorine atom in position 2 of the quinoline nucleus of these compounds was easily displaced by a variety of nucleophilic reagents (Scheme 2) such as NaOH, amines, and sodium azide. In particular, the reaction of **6q** with NaOH in dioxane led to the contemporary hydrolysis of both the ester and the iminochloride function (compound **4s**), while the reaction of **6x** with sodium azide gave, after hydrolysis, the tetrazoloquinoline derivative **4n**. It is noteworthy that the reaction of iminochlorides **6q**,**x**,**y** with glycine ethyl ester hydrochloride in pyridine gave the corresponding 2-aminoquinoline derivatives, which were hydrolyzed into the amino acid derivatives **4e**,**t**,**w**. Stille cross-coupling[11] of **6q** with tetramethylstannane gave, after hydrolysis, the expected 2-methylquinoline derivative **4r**. The acylsulfonamide **4u** was synthesized by reaction of the carboxylic acid **4p** with *p*-nitrobenzensulfonamide

Scheme 5[a]

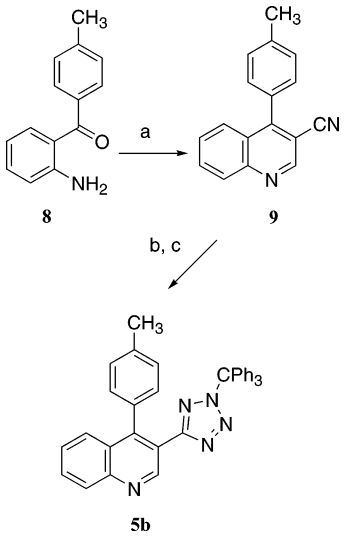

[a] Reagents: (a) $CNCH_2CH(OCH_3)_2$, PTSA, toluene; (b) $(CH_3)_3SnN_3$, xylene, (c) Ph_3CCl, NaOH, THF, CH_2Cl_2.

Scheme 6[a]

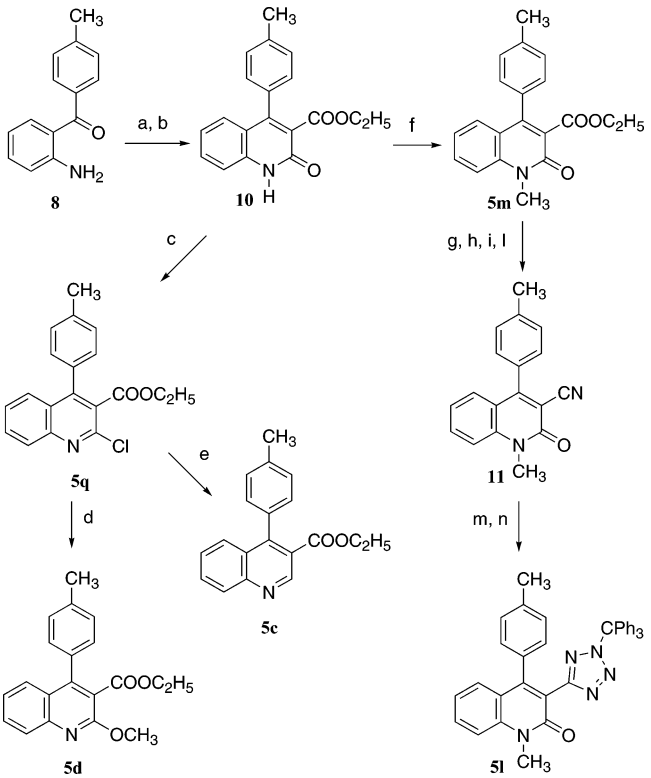

[a] Reagents: (a) $C_2H_5OCOCH_2COCl$, CH_2Cl_2; (b) NaH, C_2H_5OH; (c) $POCl_3$; (d) CH_3ONa, CH_3OH; (e) H_2, Pd/C, $(C_2H_5)_3N$, C_2H_5OH; (f) CH_3I, KOH, $(C_4H_9)_4NBr$, THF, DMF; (g) NaOH, C_2H_5OH, (h) $SOCl_2$; (i) NH_3, CH_2Cl_2; (l) $POCl_3$, C_6H_6; (m) $(CH_3)_3SnN_3$, xylene; (n) Ph_3CCl, NaOH, THF, CH_2Cl_2.

Scheme 7[a]

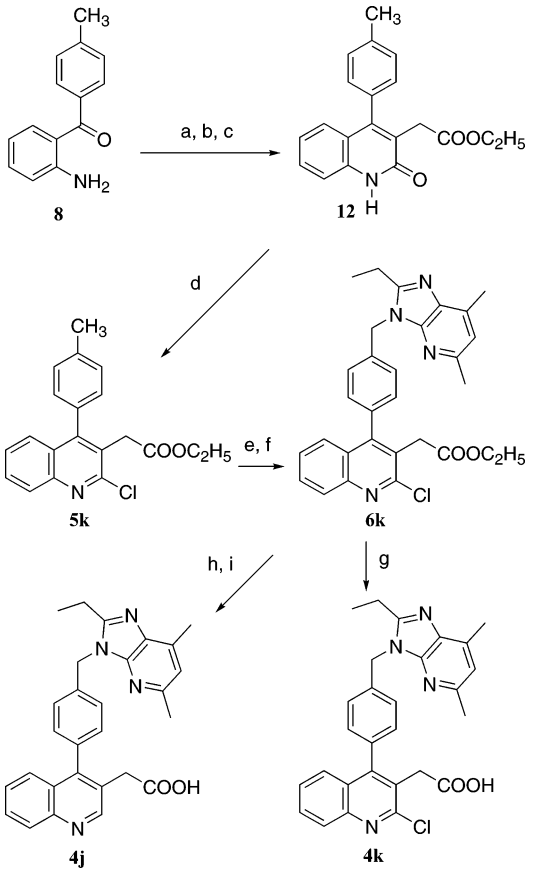

[a] Reagents: (a) $C_2H_5OCOCH_2CH_2COCl$, CH_2Cl_2; (b) NaH, C_2H_5OH, (c) C_2H_5OH, $POCl_3$; (d) $POCl_3$; (e) NBS, dibenzoyl peroxide, CCl_4; (f) 5,7-dimethyl-2-ethyl-3*H*-imidazo[4,5-*b*]pyridine, NaH, DMF; (h) H_2, Pd/C, $(C_2H_5)_3N$, C_2H_5OH, (i) NaOH, C_2H_5OH; (g) NaOH, THF.

Scheme 8[a]

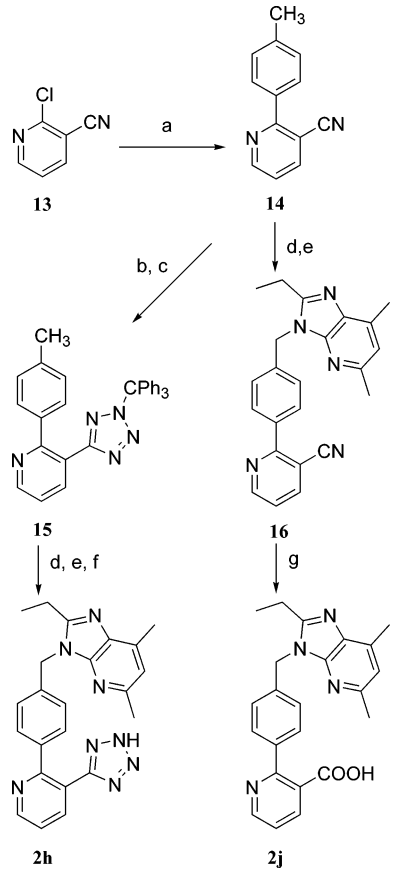

[a] Reagents: (a) *p*-$CH_3C_6H_4B(OH)_2$, K_2CO_3, $Pd(PPh_3)_2Cl_2$, DMF; (b) $(CH_3)_3SnN_3$, xylene; (c) Ph_3CCl, NaOH, THF, CH_2Cl_2; (d) NBS, dibenzoyl peroxide, CCl_4; (e) 5,7-dimethyl-2-ethyl-3*H*-imidazo[4,5-*b*]pyridine, NaH, DMF; (f) HCOOH; (g) NaOH, $HOCH_2CH_2OH$.

in the presence of EDCI and DMAP (Scheme 3). The intermediates **5a**−**d**,**k**−**m**,**q** required for the synthesis shown in Scheme 1 were prepared by means of either the classical biaryl chemistry or the 4-phenylquinoline chemistry. For example, naphthalene derivative **5a** was prepared by aryl coupling with heterogeneous palladium catalyst[12] as depicted in Scheme 4, while 3-tetrazolylquinoline intermediate **5b** was obtained by means of a three-step procedure involving the acid-catalyzed Friedländer condensation of the aminobenzophenone **8**[13] with 3,3-dimethoxypropionitrile[14] followed by the classical tetrazole chemistry (Scheme 5), and quinoline intermediates **5c**,**d**,**l**,**m**,**q** were synthesized by means of the standard procedures shown in Scheme 6.[15]

3-Quinolineacetic acid derivatives **4j**,**k** were obtained (Scheme 7) from the common intermediate **6k** possessing a chlorine atom in position 2 of the quinoline nucleus. This chlorine was demonstrated to be necessary, from the point of view of the synthesis, because the attempts at applying the bromination-coupling procedure (successfully employed in the case of 3-quinolinecarboxylate **5c**) to the higher homologue ethyl 4-(4-methylphenyl)-3-quinolineacetate were unsuccessful. The difference between these two compounds consisted of the attachment of the carboxylic group to the quinoline nucleus and, consequently, the presumably higher electron-withdrawing effect of the carboxylic ester conjugated to the heteroaromatic ring. Probably, the chlorine in position 2 of the quinoline nucleus played a key role in lowering the basicity of the quinoline nitrogen atom of **5k** and prevented the self-condensation of the corresponding bromide.

Finally, reference compounds **2a**,**b**,**h**−**j** were synthesized in our laboratories following (or modifying, see Scheme 8) the procedures described by Mantlo and coworkers.[6,8,10,16]

Structural Studies

X-ray crystallographic studies were carried out on compounds **4d**, **6n**, and **6q** (Table 1, Figures 1−3). While the asymmetric units of **6n** and **6q** are formed by one molecule, in the case of **4d** they consist of two molecules showing different conformational parameters. In all the compounds, the heterocyclic systems are planar. The largest deviation from planarity is shown by the tetrazoloquinoline system in **6n** where C(6) and C(9) show the largest deviations (0.077(5) and 0.075(5)Å, respectively, from two opposite sides) from the least squares plane defined by the 13 atoms. The C═O group at position 3 of the quinoline nucleus of **6q** shows a perpendicular orientation with respect to the plane of the quinoline, as in the case of the two independent molecules of **4d**, while in compound **6n** it is almost coplanar with the quinoline (Table 2). To minimize steric hindrance, in each compound the three rings are nearly perpendicular to one another (Table 2). The phenyl ring bridging the two heterocyclic systems forms dihedral angles with the quinoline moiety in the range 65.93(12)° (**6n**) ÷ 84.85(7)° (**4d**).

Table 1. Crystal Data for Compounds **4d** and **6n**,**q**

	4d	6n	6q
formula	$C_{28}H_{26}N_4O_3 \cdot 0.5H_2O \cdot 0.5C_2H_5OH$	$C_{29}H_{27}N_7O_2$	$C_{30}H_{29}ClN_4O_2$
MW	498.57	505.58	513.02
crystal system	triclinic	triclinic	triclinic
space group	*P*-1 (no. 2)	*P*-1 (no. 2)	*P*-1 (no. 2)
a/Å	13.641(4)	8.515(3)	9.311(1)
b/Å	14.136(1)	9.849(2)	9.917(1)
c/Å	14.302(1)	15.826(4)	15.653(1)
α/°	72.61(1)	95.45(1)	104.30(1)
β/°	83.37(1)	99.24(2)	105.96(1)
γ/°	88.93(1)	104.56(3)	97.04(1)
U/Å^3	2613.8(8)	1255.2(6)	1318.1(2)
temperature/K	293(2)	293(2)	293(2)
Z	4	2	2
F(000)	1056	532	540
D_c/g cm^{-3}	1.267	1.338	1.293
μ(Mo-K_α)/mm^{-1}	0.086	0.088	0.180
scan mode	$\omega/2\theta$	$\omega/2\theta$	$\omega/2\theta$
scan range/°	$1 \le \theta \le 25$	$1 \le \theta \le 25$	$1 \le \theta \le 25$
scan width/°	1.26	1.00	0.92
scan speed/ deg min^{-1}	3	3	3
independent reflections	6757	4409	4569
obsd reflections ($I > 2\sigma(I)$)	5255	1943	3715
no. parameters refined	712	373	355
R_1 ($I > 2\sigma(I)$)	0.046	0.070	0.044
wR_2 ($I > 2\sigma(I)$)	0.112	0.133	0.113

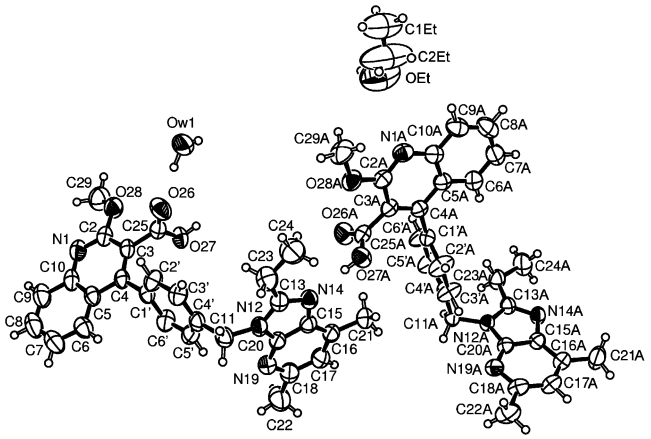

Figure 1. Crystal structure of **4d**. Ellipsoids enclose 50% of probability. The OH group of the ethanol having site occupation factor of 0.62(1) is reported.

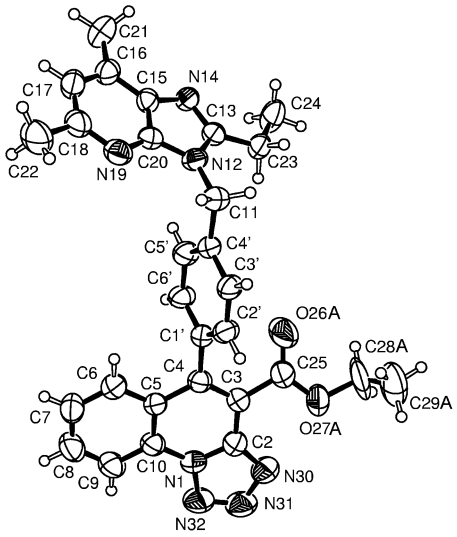

Figure 2. Crystal structure of **6n**. Ellipsoids enclose 50% of probability. The atom O(26) and the OEt group having site occupation factor of 0.60(1) are reported.

Interestingly, the analysis of the crystal packing of the carboxylic acid derivative **4d** shows the presence of a complex hydrogen bonding network. This is due to the simultaneous presence of heterocyclic nitrogen atoms and of one COOH group in the structure of **4d**, and of one molecule of water and one of ethanol in the asymmetric unit. In particular, the cocrystallized water molecule [OW1 (*x*, *y*, *z*)] establishes hydrogen bonds with both the lutidine nitrogen atom of the same asymmetric unit [N(19A) (*x*, *y*, *z*)] and the carbonyl oxygen atom of **4d** belonging to another asymmetric unit [O(26) ($1 - x$, $-y$, $1 - z$)]. Another hydrogen bond interaction is present between the COOH group [O(27) (*x*, *y*, *z*)] and the imidazole nitrogen atom N(14A) (x, $-1 + y$, z), while O(27A) interacts with (N14). The OH group [OEt (*x*, *y*, *z*)] of the ethanol forms a hydrogen bond with quinoline nitrogen N(1A) (x, y, $-1 + z$). The distances (H)O···N are in the range 2.59 ÷ 3.16Å (Figure 1). Thus, these results show that all the heterocyclic (imidazole, lutidine, and quinoline) nitrogen atoms possessing one unshared lone pair behave as hydrogen bonding acceptors in the crystal.

Structure−Affinity Relationship Studies

The newly synthesized bicyclic derivatives **4** (showing a suitable degree of purity as confirmed by ^{1}H NMR and combustion analyses) were tested for their potential ability to displace [^{125}I]Sar^1,Ile^8-Ang II specifically bound to AT_1 receptor in rat hepatic membranes, in comparison with reference monocyclic compounds **2a**,**b**,**h**−**j**, losartan, and valsartan, following well-established protocols.[17] The results of the binding stud-

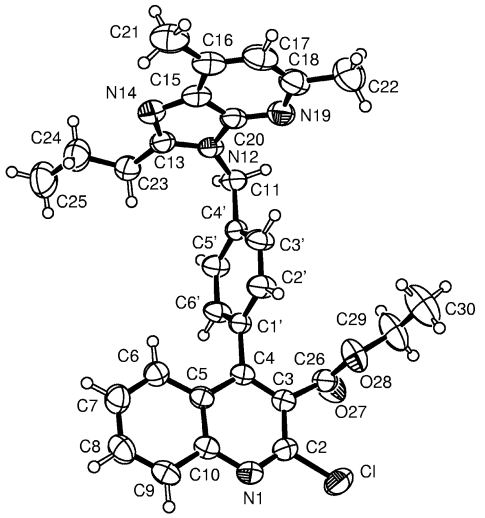

Figure 3. Crystal structure of **6q**. Ellipsoids enclose 50% of probability.

ies summarized in Table 3 show that most of the tested compounds displayed high affinity for AT_1 receptor. The most potent compounds **4b**,**q**,**r**,**t** can be considered equipotent with losartan.

(a) Effects of the Modification of the Distal Phenyl Ring. The introduction of an additional benzene ring in the structure of carboxylic acid derivative **2i** leading to naphthalene derivative **4a**[18] appeared to be tolerated by the receptor. Moreover, the transformation of the naphthalene moiety of carboxylic derivative **4a** into the quinoline one of **4c** seemed to have slightly positive effects, as the AT_1 receptor affinity of **4c** was twice as higher as that of its carbaisostere **4a**.

The latter result appeared to be in disagreement with those described by Mantlo et al.[8] for compounds **2** and with those obtained by Reitz[7] and co-workers with compounds **3**. These authors showed that the replacement of CH to N in the distal phenyl of compounds **2c** or **3a** produced more or less pronounced decreases in the AT_1 receptor affinity (see Chart 2). It is noteworthy that the comparison of the affinities of the monocyclic derivatives **2a**,**h**−**j**, which we used as reference compounds, confirmed the trend described in the literature.[7,8]

(b) Effects of the Modification of the Acidic Moiety. While in the series of the reference monocyclic compounds **2a**,**h**−**j** the replacement of the tetrazole moiety of compounds **2a** and **2h** with a carboxyl group (leading to **2i** and **2j**, respectively) produced a decrease in the receptor affinity of about 1 order of magnitude (this effect was comparable with that reported in the literature for losartan[19]), in the series of bicyclic derivatives **4** the carboxyl and tetrazole groups appeared to be completely bioisosteric acidic moieties.

The transformation of the carboxyl group of **4p** into an acylsulfonamide group of compound **4u** led to an affinity decrease of 1 order of magnitude, in disagreement with that described in the literature concerning some monocyclic derivatives.[19] Similarly, the insertion of a methylene spacer between the acidic moiety and the quinoline nucleus, as in quinoline-3-acetic acid derivative **4j**, decreased the affinity by more than 1 order of magnitude.

(c) Effects of the Introduction of a Substituent in the Ortho-Position with Respect to the Acidic Moiety. The introduction of a substituent in the ortho-position with respect to the acidic moiety produced different effects which appeared to be dependent on the stereoelectronic characteristics of the substituent (and on the potential interaction with the acidic moiety). Replacement of the hydrogen atom with NH_2 group appeared to be well tolerated by the receptor (compare **4c**,**p**,**v** with **4e**,**t**,**w**, respectively), while the increase in steric bulk in the series of alkyl-substituted amino derivatives **4e**−**i** led to a progressive decrease in the receptor affinity. Other small substituents possessing different electronic characteristics such as a methyl group and a chlorine atom appeared to have only slight effects (compare **4p** with **4r**,**q**), while the introduction of a hydroxy group dramatically decreased the receptor affinity (compare **4p** vs **4s**). The low affinity shown by hydroxy derivative **4s** is not surprising provided its probable prototropic side chain tautomerism to the oxo-form[20] and the similarly low affinity shown by 1-methyl-2-quinolinone derivative **4m** are taken into account together. Interestingly, the transformation of the quinoline nucleus of our compounds into 1-methyl-2-quinolinone is more negative in the case of tetrazole derivative **4l** (compare **4l** vs **4b**) than in the case of carboxylic acid derivative **4m** (compare **4m** vs **4c**). Finally, the introduction of either a methoxy group (compound **4d**) or of a condensed tetrazole ring (**4n**) led to a slight (but significant) decrease in the receptor affinity.

(d) Effects of the Modification of the Lipophilic Substituent in Position 2 of the Imidazo[4,5-*b*]-pyridine Nucleus. The work performed on losartan congeners has shown the importance of a short alkyl chain at position 2 of imidazole, fused imidazole, or

Table 2. Conformational Parameters for **6n**,**q** and **4d**

torsion angle (deg)	**4d** Mol 1	**4d** Mol 2	**6q**	**6n**
C(2)−C(3)−C=O	92.2(3)	96.4(3)	84.4(3)	147(1)
C(3)−C(4)−C(1′)−C(2′)	−110.0(3)	−82.6(3)	−77.6(2)	−66.9(6)
C(3′)−C(4′)−C(11)−N(12)	80.0(3)	−67.1(3)	−60.0(2)	178.7(4)
N(12)−C(13)−CH_2−C	−178.5(3)	−179.0(2)	−175.9(2)	179.0(4)

dihedral angle between planes (deg)	**4d** Mol 1	**4d** Mol 2	**6q**	**6n**
1, 2	69.42(7)	84.85(7)	76.92(5)	65.93(12)
1, 3	85.79(4)	75.31(5)	75.88(4)	66.37(9)
2, 3	63.17(7)	74.59(6)	80.57(4)	82.64(11)

[a] Least squares planes defined as 1: N1−C10 (10 atoms); 2: C1′−C6′ (six atoms); 3: N12−C20 (nine atoms).

Table 3. AT_1 Receptor Binding Affinities and Inhibition of Ang II-Induced Contraction in Rabbit Aortic Strips of Compounds **2** and **4**

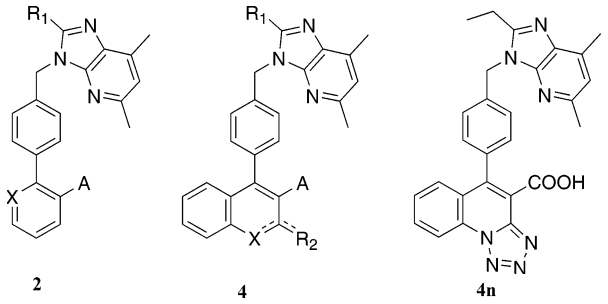

2 **4** **4n**

						rabbit aortic strips IC_{50} (nM)	
compd	X	R_1	R_2	A	binding IC_{50} (nM) ± SEM[a]	60 min	120 min[b]
2a	CH	C_2H_5		CN_4H	0.4 ± 0.1		
2b	CH	*n*-C_3H_7		CN_4H	0.8 ± 0.01		
2h	N	C_2H_5		CN_4H	18 ± 2.9		
2i	CH	C_2H_5		COOH	10 ± 2.2		
2j	N	C_2H_5		COOH	819 ± 151		
4a	CH	C_2H_5	H	COOH	33 ± 4.7		
4b (C*R*3210)	N	C_2H_5	H	CN_4H	6.9 ± 1.3	4.0	2.0
4c	N	C_2H_5	H	COOH	17 ± 1.8		
4d	N	C_2H_5	OCH_3	COOH	74 ± 6.4		
4e	N	C_2H_5	NH_2	COOH	13 ± 1.2		
4f	N	C_2H_5	$NHCH_3$	COOH	13 ± 1.9		
4g	N	C_2H_5	$N(CH_3)_2$	COOH	29 ± 4.4		
4h	N	C_2H_5	NH*n*-C_3H_7	COOH	66 ± 4.1		
4i	N	C_2H_5	N(*n*-C_3H_7)$_2$	COOH	492 ± 85		
4j	N	C_2H_5	H	CH_2COOH	576 ± 104		
4k	N	C_2H_5	Cl	CH_2COOH	215 ± 40		
4l	NCH_3	C_2H_5	=O	CN_4H	> 300		650
4m	NCH_3	C_2H_5	=O	COOH	326 ± 36		170
4n					52 ± 6.4		
4o	N	*n*-C_3H_7	H	CN_4H	12 ± 2.1		
4p	N	*n*-C_3H_7	H	COOH	11 ± 1.8		
4q	N	*n*-C_3H_7	Cl	COOH	7.7 ± 1.0		
4r	N	*n*-C_3H_7	CH_3	COOH	9.0 ± 1.6	13	
4s	N	*n*-C_3H_7	OH	COOH	261 ± 65		
4t	N	*n*-C_3H_7	NH_2	COOH	4.2 ± 0.34	3.3	
4u	N	*n*-C_3H_7	H	$CONHSO_2C_6H_4(p)NO_2$	106 ± 19		
4v	N	*n*-C_4H_9	H	COOH	41 ± 7.1		
4w	N	*n*-C_4H_9	NH_2	COOH	13 ± 1.5		
Ang II					0.4 ± 0.1		
losartan					6.7 ± 0.5	9.9	
valsartan					1.9 ± 0.2		

[a] Each value is the mean ± SEM of three determinations and represents the concentration giving half the maximum inhibition of [^{125}I]Sar^1,Ile^8-Ang II specific binding to rat hepatic membranes. [b] The antagonism of Ang II-contracted rabbit aorta rings was assayed by using different time of contact of the tested compound.

equivalent moieties for the binding efficiency.[21] In the class of imidazopyridine derivatives **2**, ethyl and *n*-propyl groups have been described to be fully equivalent from the point of view of the receptor affinity.[6a] Accordingly, ethyl derivative **2a** showed in our test system a 2-fold higher affinity with respect to propyl derivative **2b**. A similar SAFIR trend was found for the couple of bicyclic tetrazole derivatives **4b** and **4o**, while a small deviation from this trend was observed in the case of the short series of carboxylic derivatives **4c**,**p**,**v** and amino derivatives **4e**,**t**,**w**. Indeed, in both series the optimal lipophilic substituent appeared to be the *n*-propyl group.

Computational Studies on the Isolated Ligands

The results of the computational analysis carried out on selected isolated anionic ligands are summarized in Figure 4. The electrophilic superdelocalizability[22] on the acidic moieties and on the adjacent aromatic rings has been chosen as a descriptor of the ligand propensity to establish charge-reinforced hydrogen bond interactions with a basic (protonated) residue of the receptor and dispersive interactions with suitable receptor aromatic residues, respectively. The use of this descriptor furnished a semiquantitative rationalization of the structure−affinity relationship data. In fact, both the replacement of the tetrazole moiety with the carboxyl group and the introduction of a nitrogen atom in the monocyclic ligands **2a**,**h**−**j** (Figure 4, top) produce a significant reduction of the superdelocalizability characterizing the acidic moiety. This effect is less marked for the ligands carrying the quinoline framework.

No significant variations were observed for the electrophilic superdelocalizability calculated on the aromatic/heteroaromatic rings (moiety **b** and **c**, in Figure 4). In fact, the localization of the electronic cloud on the highest occupied molecular orbital (HOMO) of **2h**,**j** is very similar to that of their analogues **2a** and **2i**, respectively, and the great difference in the value of this index is shown by compounds **2h** and **2j**. It is worth

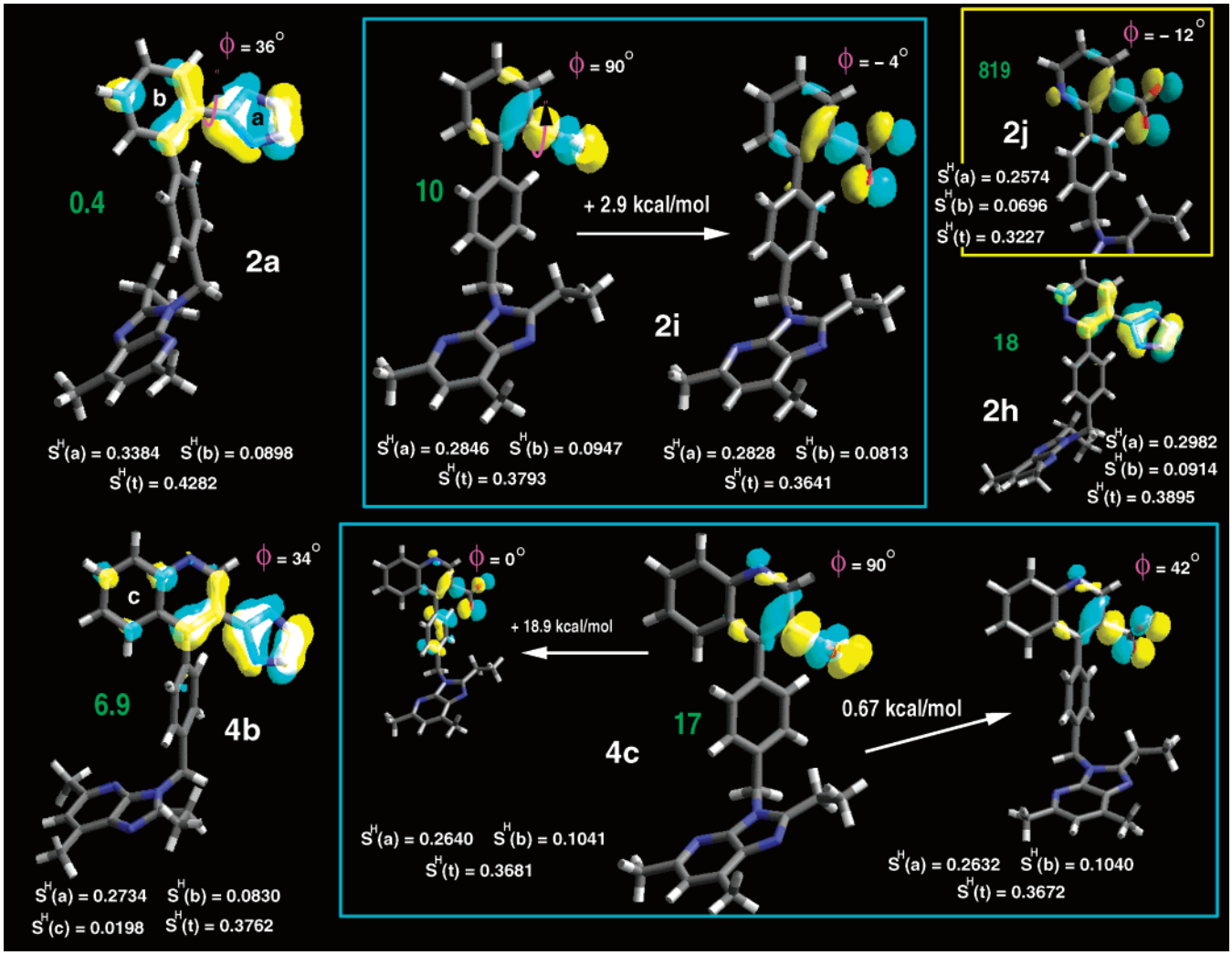

Figure 4. Electrophilic Superdelocalizability on the acidic moiety (**a**: $S^H(a)$), on the adjacent aromatic/heteroaromatic rings (**b**: $S^H(b)$, and **c**: $S^H(c)$), and on the overall antagonist molecule where the highest occupied molecular orbital (HOMO) is localized ($S^H(t)$). Binding affinities data values (IC_{50}) are reported in green. The value of the dihedral angle (ϕ) which regulates the mutual position of the acidic moiety and the aromatic/heteroaromatic ring is reported, and the most significant energetic conformers of the ligands are shown.

noting that this molecular index is relatively independent of molecular conformation, at least in the conformational range considered to be accessible by the ligands when interacting with the receptor. Indeed, the lowest energy conformation of compounds **2i** and **4c** shows the carboxylic anionic moiety perpendicular to the aromatic/heteroaromatic rings ($\phi = 90°$). Cheap energetic costs have to be spent by these ligands (2.9 and 0.67 kcal/mol, respectively) to achieve a local minimum in which the carboxylic moiety tends to be more coplanar with the aromatic/heteroaromatic rings and to show higher similarity with the tetrazole conformational preference (see Figure 4). A different behavior is observed when the energy necessary to force the acidic moiety in a planar conformation is higher, as shown at the bottom of Figure 4 for the $\phi = 0°$ conformer of ligand **4c**.

An additional important observation suggested from the analysis of the electrophilic superdelocalizability is that the frontier orbital electronic cloud of the neutral compound shifts from the carboxylic moiety to the imidazo[4,5-*b*]pyridine nucleus, as shown at the bottom of Figure 5. This supports the hypothesis of a two-step binding mechanism: the first step is controlled by a long-range electrostatic interaction for both agonists and antagonists; in the second step short-range intermolecular interactions established by the imidazo[4,5-*b*]-pyridine moiety dictated the functional profile of the ligands, as suggested by single point mutagenesis studies on the receptor.[23]

Computational Studies on the Ligand−Receptor Complexes

The three-dimensional receptor model constructed at the beginning of this study was based on both the bacteriorhodopsin structure[24] and on the helical wheel projection model proposed by Baldwin.[25] Although approximate, the model was instrumental in guiding the synthesis of new ligands designed to explore the molecular basis of receptor interaction.

The model we present here has been updated according to the recently determined 2.8 Å X-ray structure of rhodopsin.[26] The residues considered to form the surface of the binding site for the antagonists **2** and **4** are L70 (Helix 2), **S105**, **V108**, **S109**, **N111**, L112, Y113, **S115**, V116 (Helix 3), A159, S160, **A163** (Helix 4), Y170, V179, A181 (II Extracellular loop), L195, **K199**, G203, F204, F208 (Helix 5), F249, **S252**, **W253**, **V254**, **P255**, **H256**,

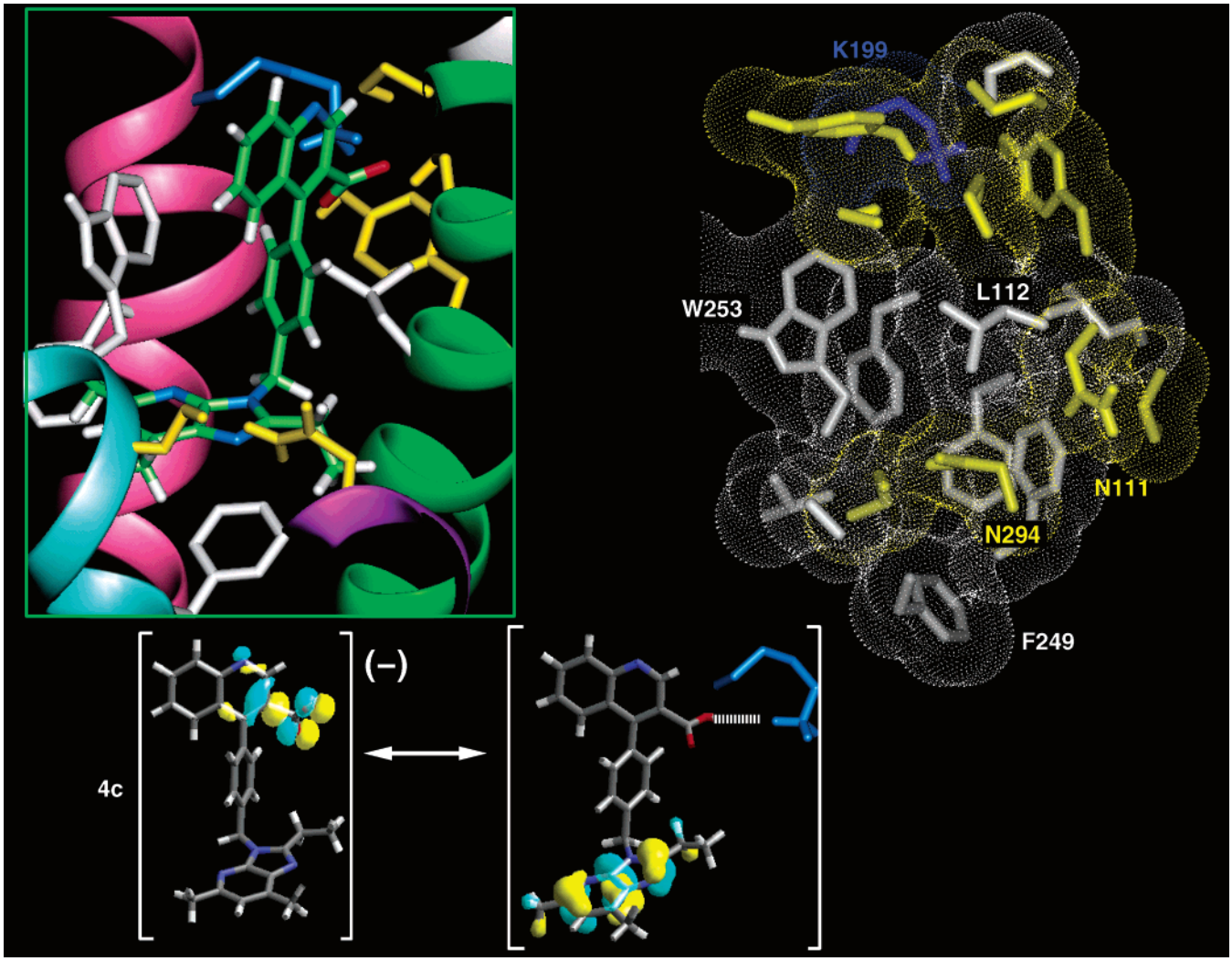

Figure 5. Minimized average structure of the **4c**−AT_1 receptor complex (top left), detailed view of the antagonist binding site (top right), and modification of the HOMO orbital upon neutralization of the anionic **4c** inhibitor (bottom).

T260 (Helix 6), **A291**, **F293**, **N294**, **N295**, L297 (Helix 7). The residues reported in bold capitals have been demonstrated (by means of site-directed mutagenesis studies) to be important for binding,[23] and some of these establish common key interactions with peptide agonists and nonpeptide antagonits.[27]

The essential shape and physicochemical characteristics of the receptor cavity assumed to accommodate ligands **2** and **4** is shown in Figure 5 (top right). The back- and bottom-walls are constituted by hydrophobic residues, while polar residues are situated at the top of the cavity, where the basic **K199** residue lies, and spotted the front wall at a depth from **K199** of about 8−10 Å which is perfectly congruent with the distance between the antagonist acidic moiety and the imidazo-[4,5-*b*]pyridine nucleus. Therefore, in a dynamic view, the hydrogen bonding acceptor propensity of the antagonist pendant heterocyclic moiety could be satisfied alternatively by the **N111**, or **N294**, or **S252** residues, once the main ion-pair interaction has been achieved. The energy minimized average structure of the **4c**−AT_1 receptor complex is shown in Figure 5.

Functional Studies

Some selected compounds showing different binding affinities were evaluated for antagonism of Ang II-induced contraction in rabbit aortic strips.[17,28] The results (Table 3) show that all the tested compounds behaved as Ang II antagonists in this functional model showing IC_{50} values well related to their binding affinities. The most potent compounds in the binding test **4b**,**t** were highly potent in inhibiting Ang II-induced contraction. Indeed, 2-amino-3-quinolinecarboxylic acid derivative **4t** and tetrazole derivative **4b** were slightly more active than losartan. Moreover, the potency of compound **4b** was enhanced when the contact with the antagonist was increased from 60 to 120 min.

Discussion

Among the AT_1 receptor antagonists bearing a nitrogen atom in the biphenyl skeleton, compound **2f** represented an interesting starting point for the design of new antihypertensive agents. It was reported both to show an affinity just four times lower than its carbaisostere **2c** and to be an orally active Ang II antagonist showing a somewhat poorer oral bioavailability (probably for the decreased lipophilicity) than that of **2c**.[8] This observation, together with the complex effects of the introduction of a nitrogen atom in the biphenyl moiety (see the Introduction), led to the design of compound **4b** and its derivatives with the aim of both developing new antihypertensive agents and under-

standing the molecular basis of their pharmacodynamic and pharmacokinetic properties. We believed that the introduction of the fused benzene ring should ensure the lipophilicity necessary for a good oral bioavailability, and the SAFIR study involving compounds **4** should provide information on the ligand−AT_1 receptor interaction.

Very interestingly, quinoline derivative **4b** (C*R*3210) showed AT_1 receptor affinity in the low nanomolar range very similar both to that described for pyridine derivative **2f** and to that shown by losartan. Moreover, **4b** was slightly more active than losartan in inhibiting Ang II-induced contraction in rabbit aortic ring, and therefore it was considered to be an interesting candidate for further preclinical studies. Thus, the pharmacokinetic properties of **4b** and some selected members of this class of AT_1 antagonists are under evaluation in a comprehensive study devoted to the understanding of their structure−pharmacokinetics relationships.

The SAFIR analysis performed on our compounds revealed that the introduction of a nitrogen atom in the naphthalene derivative **4a** to give quinolinecarboxylic acid **4c** is well tolerated by the receptor. The presence of the additional condensed benzene ring of compounds **4a**−**w** has little consequences on the receptor affinity (compare **4a** with **2i**), but it appears to produce some peculiarities in key SAFIR trends. For example, in the series of bicyclic derivatives **4**, the carboxylic and tetrazole groups appeared to be completely bio-equivalent acidic moieties, while the monocyclic tetrazole derivatives **2a** and **2h** were found more than 1 order of magnitude more potent than corresponding monocyclic carboxylate derivatives **2i** and **2j**, respectively (in agreement with the results described for losartan). These results can be rationalized by considering the electrophilic superdelocalizability computed over the antagonist moiety where the HOMO orbital is localized. In fact, the reactivity potential of the different acidic moieties in the series of ligands **4** is almost identical, while the carboxylic anionic head is significantly less reactive than the tetrazole moiety in compounds **2** (Figure 4). From a qualitative point of view, the shape of the electronic cloud distribution on the highest occupied molecular orbital does not show significant differences among the compounds (Figure 4); however, the value of the reactivity index gives a rough but useful classification of the ligands with respect to their binding activities: subnanomolar ligands possess a total electrophilic superdelocalizability ($S^H(t)$) of about 0.43. For nanomolar ligands, this index ranges in the interval 0.36−0.40; finally, micromolar ligands show a $S^H(t)$ value of about 0.32.

Further insight into the molecular basis of the interactions can be obtained by a dynamic analysis of the inhibitor−receptor complexes. Figure 5 shows the minimized average structure of the **4c**−AT_1 receptor complex, a detailed view of the binding site, and the modification of the HOMO orbital upon neutralization of the anionic antagonist **4c**. The putative antagonist binding site is essentially hydrophobic, the only basic residue being K199, which has been identified to be the key residue for agonist and antagonist recognition.[29] The overall information obtained justifies the hypothesis that a long-range electrostatic interaction controls the preliminary recognition step and is shared by agonists and antagonists. The second step differentiates the functional activity of ligands. In the case of the antagonists presented here, short-range intermolecular interactions of the imidazopyridine moiety with residues **N111**, or **N294**, or **S252** (according to the molecular framework of the ligand) perturb the hydrogen bonding network which allows the communication among helices and therefore receptor activation and signal transduction.

Experimental Section

Melting points were determined in open capillaries on a Gallenkamp apparatus and are uncorrected. Microanalyses were carried out using a Perkin-Elmer 240C elemental analyzer. Merck silica gel 60 (70−230 or 230−400 mesh) was used for column chromatography. Merck TLC plates, silica gel 60 F_{254}, were used for TLC. ^{1}H NMR spectra were recorded with a Bruker AC 200 spectrometer in the indicated solvents (TMS as internal standard): the values of the chemical shifts are expressed in ppm and the coupling constants (*J*) in Hz. Mass spectra (EI, 70 eV) were recorded either on a VG 70-250S spectrometer (Centro di Analisi e Determinazioni Strutturali, Università di Siena) or Varian Saturn 3 (Dipartimento Farmaco Chimico Tecnologico, Università di Siena). NMR spectra and elemental analyses were performed in the Dipartimento Farmaco Chimico Tecnologico, Università di Siena.

Preparation of Target Tetrazole Derivatives 4b,l,o (Deprotection of the Trityl-Protected Tetrazole Derivatives). A mixture of the appropriate trityl-protected tetrazole derivative (1.0 mmol) with formic acid (15 mL) was stirred at room temperature under argon for a suitable time (2−44 h), and the reaction progress was monitored by TLC. When the trityl-protected tetrazole derivative disappeared from the chromatogram, the reaction mixture was evaporated under reduced pressure. Purification of the residue by washing with diethyl ether gave the target compounds showing a suitable degree of purity as confirmed by ^{1}H NMR and combustion analyses.

4-[4-[(5,7-Dimethyl-2-ethyl-3*H*-imidazo[4,5-*b*]pyridin-3-yl)methyl]phenyl]-3-(2*H*-tetrazol-5-yl)quinoline (4b). The title compound was prepared from **6b** to obtain a white crystalline solid (0.36 g, 78%) melting at 257−259 °C. ^{1}H NMR ($CDCl_3$): 1.20 (t, *J* = 7.5, 3H), 2.56 (s, 3H), 2.61 (s, 3H), 2.82 (q, *J* = 7.5, 2H), 5.57 (s, 2H), 6.93 (s, 1H), 7.25 (m, 4H), 7.52 (m, 2H), 7.79 (m, 1H), 8.22 (d, *J* = 8.3, 1H), 9.53 (s, 1H). Anal. ($C_{27}H_{24}N_8 \cdot 0.5H_2O$) C, H, N.

4-[4-[(5,7-Dimethyl-2-ethyl-3*H*-imidazo[4,5-*b*]pyridin-3-yl)methyl]phenyl]-1-methyl-3-(2*H*-tetrazol-5-yl)- 2(1*H*)-quinolinone (4l). The title compound was prepared from **6l** to obtain a white crystalline solid (0.34 g, 69%) melting at 270−272 °C. ^{1}H NMR ($CDCl_3$): 1.38 (t, *J* = 7.6, 3H), 2.61 (s, 3H), 2.63 (s, 3H), 2.90 (q, *J* = 7.6, 2H), 3.93 (s, 3H), 5.59 (s, 2H), 6.89 (s, 1H), 7.22 (m, 6H), 7.52 (d, *J* = 8.4, 1H), 7.68 (m, 1H). Anal. ($C_{28}H_{26}N_8O \cdot 0.67H_2O$) C, H, N.

4-[4-[(5,7-Dimethyl-2-propyl-3*H*-imidazo[4,5-*b*]pyridin-3-yl)methyl]phenyl]-3-(2*H*-tetrazol-5-yl)quinoline (4o). The title compound was prepared from **6o** to obtain a white crystalline solid (0.37 g, 78%, mp 236−238 °C). ^{1}H NMR ($CDCl_3$): 0.89 (t, *J* = 7.5, 3H), 1.65 (m, 2H), 2.57 (s, 3H), 2.61 (s, 3H), 2.80 (t, *J* = 7.4, 2H), 5.57 (s, 2H), 6.93 (s, 1H), 7.28 (m, 4H), 7.52 (m, 2H), 7.78 (m, 1H), 8.22 (d, *J* = 8.4, 1H), 9.51 (s, 1H). Anal. ($C_{28}H_{26}N_8$) C, H, N.

Preparation of Target Carboxylic Acid Derivatives 4a,c−k,m,p−t,v,w (Basic Hydrolysis). To a solution of the appropriate ester (**6a**,**c**−**k**,**m**,**p**−**t**,**v**,**w**) (1.0 mmol) in the suitable solvent (ethanol, THF, dioxan, or ethylene glycol) (40 mL) was added 1 N NaOH (10 mL), and the resulting mixture was refluxed while the reaction progress was monitored by TLC. When the ester derivative disappeared from the chromatogram, the reaction mixture was evaporated under reduced pressure and diluted with water (20 mL), and the pH was

adjusted to 5−6 by addition of 1 N HCl. The precipitate was collected by filtration (or extracted with chloroform when necessary), washed with water, and dried under reduced pressure. Purification of the solid obtained by recrystallization from the suitable solvent or by washing with ethyl acetate or diethyl ether gave target carboxylic acid derivatives showing a suitable degree of purity as confirmed by ^{1}H NMR and combustion analyses.

1-[4-[(5,7-Dimethyl-2-ethyl-3*H*-imidazo[4,5-*b*]pyridin-3-yl)methyl]phenyl]-2-naphthalenecarboxylic Acid (4a). The title compound was obtained from ester **6a** by means of the basic hydrolysis procedure employing ethanol as the solvent (yield 90%, mp 245−247 °C). ^{1}H NMR (DMSO-d_6): 1.27 (t, J = 7.3, 3H), 2.53 (s, 3H), 2.54 (s, 3H), 2.84 (q, J = 7.3, 2H), 5.56 (s, 2H), 6.97 (s, 1H), 7.22 (m, 4H), 7.40 (m, 2H), 7.55 (m, 1H), 7.81 (d, J = 8.6, 1H), 8.01 (d, J = 8.4, 2H), 12.65 (br s, 1H). MS (EI): m/z 435 (M^+, 5). Anal. ($C_{28}H_{25}N_3O_2 \cdot 3H_2O$) C, H, N.

4-[4-[(5,7-Dimethyl-2-ethyl-3*H*-imidazo[4,5-*b*]pyridin-3-yl)methyl]phenyl]-3-quinolinecarboxylic Acid (4c). The title compound was obtained from ester **6c** by means of the basic hydrolysis procedure employing ethanol as the solvent (yield 98%, mp 293−295 °C). ^{1}H NMR: ($CDCl_3$): 1.00 (t, J = 7.5, 3H), 2.61 (s, 6H), 2.78 (q, J = 7.5, 2H), 5.57 (s, 2H), 6.95 (s, 1H), 7.29 (m, 4H), 7.48 (m, 2H), 7.77 (m, 1H), 8.21 (d, J = 8.3, 1H), 9.39 (s, 1H). Anal. ($C_{27}H_{24}N_4O_2 \cdot H_2O$) C, H, N.

4-[4-[(5,7-Dimethyl-2-ethyl-3*H*-imidazo[4,5-*b*]pyridin-3-yl)methyl]phenyl]-2-methoxy-3-quinolinecarboxylic Acid (4d). This compound was obtained from ester **6d** by means of the basic hydrolysis procedure employing ethanol as the solvent and was recrystallized from ethanol to obtain X-ray quality crystals (yield 72%, mp 210−211 °C). ^{1}H NMR: ($CDCl_3$): 0.88 (t, J = 7.5, 3H), 2.67 (m, 8H), 4.13 (s, 3H), 5.53 (s, 2H), 6.95 (s, 1H), 7.27 (m, 3H), 7.48 (m, 3H), 7.63 (m, 1H), 7.89 (d, J = 8.1, 1H). Anal. ($C_{28}H_{26}N_4O_3 \cdot 0.5H_2O \cdot 0.5C_2H_5OH$) C, H, N.

4-[4-[(5,7-Dimethyl-2-ethyl-3*H*-imidazo[4,5-*b*]pyridin-3-yl)methyl]phenyl]-*N*-(4-nitrophenylsulfonyl)-3-quinolinecarboxamide (4u). A mixture of **4p** (0.10 g, 0.22 mmol) in dichloromethane (20 mL) with 4-(dimethylamino)pyridine (DMAP) (0.029 g, 0.24 mmol), 4-nitrobenzenesulfonamide (0.048 g, 0.24 mmol), and 1-[3-(dimethylamino)propyl]-3-ethylcarbodiimide hydrochloride (EDCI) (0.046 g, 0.24 mmol) was stirred at room temperature for 48 h under argon. The solvent was removed under reduced pressure, and the residue was purified by flash chromatography with ethyl acetate−methanol (7:3) as the eluent to give pure **4u** as a white solid (0.093 g, yield 67%, mp 285 °C dec). ^{1}H NMR: (DMSO-d_6): 0.89 (t, J = 7.4, 3H), 1.69 (m, 2H), 2.49 (s, 6H), 2.75 (t, J = 7.5, 2H), 5.50 (s, 2H), 6.93 (s, 1H), 7.07 (m, 4H), 7.39 (m, 2H), 7.68 (m, 3H), 7.99 (d, J = 8.2, 1H), 8.10 (d, J = 8.6, 2H), 8.93 (s, 1H). MS (FAB): m/z 635 (M + 1). Anal. ($C_{34}H_{30}N_6O_5S \cdot 3H_2O$) C, H, N.

General Procedure for the Preparation of Compounds 6a−d,k−m,o−q,v,x,y (Bromination-Coupling Procedure). A mixture of the toluene derivative **5a−d,k−m,q** (1.5 mmol) in 40 mL of CCl_4 with *N*-bromosuccinimide (0.27 g, 1.5 mmol) and dibenzoyl peroxide (0.03 g, 0.12 mmol) was refluxed for a suitable time (typically 2−3 h), and the reaction progress was monitored by TLC. The initial solvent volume was reduced by half under reduced pressure, the insoluble succinimide was filtered off, and the resulting mixture was evaporated under reduced pressure. The residue was dissolved into anhydrous DMF (10 mL) and added to a mixture (aged at 0 °C for 20 min) of the appropriate 2-alkyl-5,7-dimethyl-3*H*-imidazo-[4,5-*b*]pyridine[6,10] (1.5 mmol) in anhydrous DMF (10 mL) with NaH (0.036 g, 1.5 mmol). The resulting mixture was stirred at room temperature for 15−18 h under argon, and the reaction was quenched with water (5 mL). The bulk of the DMF was evaporated under reduced pressure, and the residue was diluted with water (20 mL) and extracted with chloroform. The combined organic extracts were washed with brine, dried over sodium sulfate, and concentrated under reduced pressure. Purification of the residue by flash chromatography with ethyl acetate as the eluent gave pure compounds **6a−d,k−m,o−q,v,x,y**.

4-[4-[(5,7-Dimethyl-2-ethyl-3*H*-imidazo[4,5-*b*]pyridin-3-yl)methyl]phenyl]-3-[2-(triphenylmethyl)-2*H*-tetrazol-5-yl]quinoline (6b). The title compound was prepared from **5b** and 5,7-dimethyl-2-ethyl-3*H*-imidazo[4,5-*b*]pyridine to obtain a white solid (0.495 g, 47%) melting at 188−189 °C. ^{1}H NMR ($CDCl_3$): 1.26 (t, J = 7.6, 3H), 2.59 (s, 3H), 2.65 (s, 3H), 2.73 (q, J = 7.5, 2H), 5.39 (s, 2H), 6.92 (m, 7H), 7.04 (d, J = 8.3, 2H), 7.12 (d, J = 8.0, 2H), 7.26 (m, 9H), 7.39 (m, 2H), 7.73 (m, 1H), 8.17 (d, J = 8.5, 1H), 9.48 (s, 1H).

Ethyl 1-[4-[(5,7-Dimethyl-2-ethyl-3*H*-imidazo[4,5-*b*]pyridin-3-yl)methyl]phenyl]-2-naphthalenecarboxylate (6a). The title compound was prepared from **5a** and 5,7-dimethyl-2-ethyl-3*H*-imidazo[4,5-*b*]pyridine to obtain a white solid (0.30 g, 43%), melting at 147 °C. ^{1}H NMR ($CDCl_3$): 0.92 (t, J = 7.4, 3H), 1.38 (t, J = 7.4, 3H), 2.61 (s, 3H), 2.64 (s, 3H), 2.89 (q, J = 7.5, 2H), 4.01 (q, J = 7.0, 2H), 5.56 (s, 2H), 6.90 (s, 1H), 7.24 (m, 4H), 7.45 (m, 3H), 7.87 (m, 3H). MS (EI): m/z 463 (M^+, 100).

Ethyl 4-[4-[(5,7-Dimethyl-2-ethyl-3*H*-imidazo[4,5-*b*]pyridin-3-yl)methyl]phenyl]-3-quinolinecarboxylate (6c). The title compound was prepared from **5c** and 5,7-dimethyl-2-ethyl-3*H*-imidazo[4,5-*b*]pyridine to obtain a white solid (0.34 g, 49%), melting at 155 °C. ^{1}H NMR: ($CDCl_3$): 0.97 (t, J = 7.3, 3H), 1.38 (t, J = 7.4, 3H), 2.60 (s, 3H), 2.64 (s, 3H), 2.88 (q, J = 7.5, 2H), 4.08 (q, J = 7.2, 2H), 5.56 (s, 2H), 6.91 (s, 1H), 7.25 (m, 4H), 7.47 (m, 2H), 7.76 (m, 1H), 8.16 (d, J = 8.5, 1H), 9.31 (s, 1H).

X-ray Crystallography. Single crystals of **4d**, **6n**, and **6q** were submitted to X-ray data collection on a Siemens P4 four-circle diffractometer with graphite monochromated Mo−Kα radiation (λ = 0.71069 Å). The $\omega/2\theta$ scan technique was used for data collection.

The three structures were solved by direct methods implemented in the SHELXS-97 program.[30] The refinements were carried out by full-matrix anisotropic least-squares on F^2 for all reflections for non-H atoms by means of the SHELXL-97 program.[31]

While for **6n** and **6q** the asymmetric unit contains one molecule, in the case of **4d**, two molecules are present together with water and ethanol molecules as crystallization solvents. Statistical disorder is present for **6n** and **4d**. In the first case, disorder at the COOEt group has been treated by refining two different positions for atoms O(26), O(27), C(28), and C(29) and the attached hydrogen atoms. The refined site occupation factors are 0.60(1) for one position and 0.40(1) for the other. For **4d** statistical disorder has been found for the OH group of the cocrystallized ethanol. Two different positions have been refined with site occupation factors of 0.62(1) for one position and 0.38(1).

Biological Methods. Angiotensin II Receptor Binding Assay.[17] Male Wistar rats (Charles River, Calco, Italy) were killed by decapitation, and their livers were rapidly removed. Angiotensin II receptors from rat liver were prepared by differential centrifugation. The liver was dissected free of fatty tissue and minced accurately with small scissors, and then about 3 g of tissue was homogenized by Polytron Ultra-Turrax (maximal speed for 2 × 30 s) in ice cold 20 vol of Tris-HCl 5 mM, sucrose 0.25 M (pH 7.4). The homogenate was centrifuged at 750*g* for 10 min, and the supernatant was filtered through cheesecloth and saved. The pellets were homogenized and centrifuged as before. The combined supernatants were centrifuged at 50 000*g* for 15 min. The resulting pellet was resuspended in Tris-HCl 5 mM, sucrose 0.25 M (pH 7.4), and centrifuged as above. The final pellets were used immediately or stored frozen at −70 °C before use. The membrane pellets were resuspended in Tris-HCl 50 mM, NaCl 100 mM, $MgCl_2$ 10 mM, EDTA 1 mM, bacitracin 100 μM, PMSF 100 μM, BSA 0.1% (pH 7.4) to obtain a final protein concentration of 0.25 mg/mL. Binding of [^{125}I]Sar^1,Ile^8-angiotensin II (NEN Perkin-Elmer Life Sciences, S. A. 2000 Ci/mmol) to liver membranes was performed at 25 °C for 180 min in 96-well filtration plates

(Millipore GFB-Multiscreen). Each 250 μL incubate contained the following: [^{125}I]Sar^1,Ile^8-angiotensin II (25 pM), liver membrane proteins (25 μg) and standard or test compounds. Nonspecific binding was measured in the presence of 1 μM angiotensin II and represented 5−10% of total binding. Binding was terminated by rapid vacuum filtration using a Millipore Multiscreen device. Receptor−ligand complex trapped on filters was washed twice with 200 μL of ice cold NaCl 100 mM, $MgCl_2$ 100 mM. Dried filters disks were punched out and counted in a gamma-counter with 92% efficiency. The IC_{50} value (concentration for 50% displacement of the specifically bound [^{125}I]Sar^1,Ile^8-Angiotensin II) was estimated for the linear portion of the competition curves.

Angiotensin II Functional Antagonism in Rabbit Aorta Strips.[17] New Zealand White rabbits (3−4 kg body weight, Harlan Italy) were killed by cervical dislocation, after a slight ether anaesthesia. The descending thoracic aorta, with the endothelium removed, was cut into helical strips 3 to 4 mm wide, and 15 to 20 mm long. These strips were mounted in 20 mL tissue baths containing Krebs−Henseleit solution of the following composition (mM): NaCl 118; KCl 4.69; KH_2PO_4 1.17; $MgSO_4 \cdot 7H_2O$ 1.17; $CaCl_2 \cdot 2H_2O$ 2.51; $NaHCO_3$ 25; glucose 11.1. The tissue baths were kept at 37 °C and aerated with 95% O_2 and 5% CO_2. Each strip was connected to an isometric transducer (Basile, Italy), and a resting tension of 2 g was applied to the tissues. Changes in isometric tension were displayed on a four-channel pen recorder (Basile, Italy). The tissues were allowed to equilibrate for 1 h and were washed every 10 min. The strips were then stimulated by increasing concentrations of angiotensin II to obtain a cumulative concentration−response curve. After 30 min washout, submaximal-effect (70−80%) concentration of angiotensin II was chosen to test the inhibitory effects of the substances under study. Various concentrations of the antagonists or vehicles were added, and at least 20 min contact with the tissues was allowed before adding the agonist to the bathing fluid. The antagonist activity was expressed as percentage of inhibition of the agonist contractions. The regression line was calculated, and the concentration capable of inhibiting the effect of the agonist by 50% (IC_{50}) and its $P = 0.05$ fiducial limits were calculated from the regression line.

Computational Methods. Ligand Characterization. The structures of the ligands studied were fully optimized in their neutral and anionic forms by means of AM1[32] molecular orbital calculation, using the MOPAC package implemented in the Cerius2 program (Accelrys, San Diego, CA). The three-dimensional structure of ligand **4d**, solved by X-ray crystallography in our laboratory (see text), was taken as an input for the AM1 optimization. Conformational analysis was carried out for compounds **2a**, **2i**, **4b**, and **4c** in order to identify accessible conformers showing maximum similarity in the frontier orbital descriptors.

Comparative Modeling of the Rat AT_1 Receptor. The recently determined 2.8Å X-ray structure of rhodopsin[26] was used to build the rat AT_1 receptor model. The sequence alignment used as input for the Modeller[33] program was obtained by Clustalw[34] multiple sequence alignment of bovine rhodopsin and rat, mouse, human, rabbit, bovine, and canine AT_1 receptor sequences. Among the 50 models obtained by randomizing the Cartesian coordinates, allowing a deviation of ±4 Å, we selected the one showing the lowest restraint violations and the lowest number of poor main-chain and side-chain conformations. The quality of the models was checked by making use of the protein health module of the Quanta98 program.[35] Polar hydrogen atoms were added to the selected model, and energy minimization and dynamics were carried out by means of the CHARMM program[36] following a standard procedure consisting of 50 steps of steepest descent, followed by a conjugate gradient minimization until the rms gradient of the potential energy was lower than 0.001 kcal/molÅ. The united atom force-field parameters, a distance-dependent dielectric term ($\epsilon = 4r$), and a 12 Å nonbonded cutoff were employed. During dynamics, the lengths of the bonds involving hydrogen atoms were constrained according to the SHAKE algorithm,[37] allowing an integration time step of 0.001 ps. Moreover, weak harmonic constraints (30 kJ/mol per Å) were applied between the backbone oxygen atoms of residue i and backbone nitrogen atom of residue i+4 by means of the NOE facility in the CHARMM program[36] in order to maintain the helical structure.

The structures were thermalized to 300 K with 5 °C rise per 6000 steps by randomly assigning individual velocities from the Gaussian distribution. After heating, the systems were allowed to equilibrate until the potential energy versus time was approximately stable (34 ps). Velocities were scaled by a single factor. An additional 10 ps period of equilibration with no external perturbation was run. Time-averaged structures were then determined over the last 200 ps of each simulation.

Building and Refinement of the Ligand−Receptor Complexes. The main criteria followed to dock the ligands into the minimized average structure of the receptor were (a) the formation of a charge-reinforced hydrogen bond between the acidic (tetrazole or carboxylic) moieties of the ligands and the **K199** residue of Helix 5, (b) the achievement of a hydrogen bond between the imidazo[4.5-*b*]pyridine nucleus of the ligands and one of the following polar residues **N111** (Helix 3), **N294** (Helix 7), **S252** (Helix 6) which protrude into the receptor pore at a distance of about 8−9Å deeper than **K199**. The complexes were refined according to the procedure described in the previous paragraph.

Acknowledgment. Thanks are due to Italian MIUR for financial support. Prof. Stefania D'Agata D'Ottavi's careful reading of the manuscript is also acknowledged.

Supporting Information Available: Full experimental details for the synthesis and the characterization of compounds **4**, **2**, and their intermediates (chemistry, NMR, MS, and X-ray crystallographic details for compounds **4d**, **6n**,**q**). This material is available free of charge via Internet at http://pubs.acs.org.

References

(1) De Gasparo, M.; Catt, K. J.; Inagami, T.; Wright, J. W.; Unger, T. International Union of Pharmacology. XXIII. The Angiotensin II Receptors. *Pharmacol. Rev.* **2000**, *52*, 415−472 and references therein.

(2) Cockcroft, J. R.; Sciberras, D. G.; Goldberg, M. R.; Ritter, M. J. Comparison of Angiotensin-Converting Enzyme Inhibition with Angiotensin II Receptor Antagonism in the Human Forearm. *J. Cardiovasc. Pharmacol.* **1993**, *22*, 579−584.

(3) Unger, T. The Role of the Renin-Angiotensin System in the Development of Cardiovascular Disease. *Am. J. Cardiol.* **2002**, *89*(suppl), 3A−10A.

(4) Inoue, Y.; Nakamura, N.; Inagami, T. A Review of Mutagenesis Studies of Angiotensin II Type 1 Receptor, the Three-Dimensional Receptor Model in Search of the Agonist Binding Site and the Hypothesis of a Receptor Activation Mechanism. *J. Hypertens.* **1997**, *15*, 703−714.

(5) (a) Wexler, R. R.; Greenlee, W. J.; Irvin, J. D.; Goldberg, M. R. Prendergast, K.; Smith, R. D.; Timmermans, P. B. M. W. M. Nonpeptide Angiotensin II Receptor Antagonists: The Next Generation in Antihypertensive Therapy. *J. Med. Chem.* **1996**, *39*, 625−656. (b) Schmidt, B.; Schieffer, B. Angiotensin II AT1 Receptor Antagonista. Clinical Implications of Active Metabolites. *J. Med. Chem.* **2003**, *46*, 2261−2270, and references therein.

(6) (a) Mantlo, N. B.; Chakravarty, P. K.; Ondeyka, D. L.; Siegl, P. K. S.; Chang, R. S.; Lotti, V. J.; Faust, K. A.; Chen, T.-B.; Schorn, T. W.; Sweet, C. S.; Emmert, S. E.; Patchett, A. A.; Greenlee, W. J. Potent, Orally Active Imidazo[4,5-*b*]pyridine-Based Angiotensin II Receptor Antagonists. *J. Med. Chem.* **1991**, *34*, 2919−2922. (b) Kim, D.; Mantlo, N. B.; Chang, R. S.; Kivlighn, S. D.; Greenlee, W. J. Evaluation of Heterocyclic Acid Equivalents as Tetrazole Replacements in Imidazopyridine-Based Nonpeptide Angiotensin II Receptor Antagonists. *Bioorg. Med. Chem. Lett.* **1994**, *4*, 41−44.

(7) Reitz, D. B.; Penick, M. A.; Reinhard, E. J.; Cheng, B. K.; Olins, G. M.; Corpus, V. M.; Palomo, M. A.; McGraw, D. E.; McMahon, E. G. 1H-1,2,4-Triazole Angiotensin II Receptor Antagonists: N-Phenylpyridinylmethyl and N-Pyridinylphenylmethyl Analogues of SC-50560. *Bioorg. Med. Chem. Lett.* **1994**, *4*, 99−104.

(8) Mantlo, N. B.; Chang, R. S. L.; Siegl, P. K. S. Angiotensin II Receptor Antagonists Containing a Phenylpyridine Element. *Bioorg. Med. Chem. Lett.* **1993**, *3*, 1693−1696.

(9) As far as the pharmacokinetic properties are concerned, it should be noted that even the marketed AT_1 receptor antagonists show limited oral bioavailability (eprosartan 13%, valsartan 25%, losartan 33%, candesartan 42%, telmisartan 50%, irbesartan 60−80%). [(a) Israili, Z. H. Clinical Pharmacokinetics of Angiotensin II (AT1) Receptor Blockers in Hypertension. *J. Hum. Hypertens*. **2000**, *14* suppl 1, S73−86. (b) Brunner, H. R. The New Angiotensin II Receptor Antagonist, Irbesartan. *Am. J. Hypertens*. **1997**, *10*, 311S−317S.)] Furthermore, losartan exhibiting highly variable oral bioavailability is transported by P-glycoprotein, while its carboxylic acid metabolite is not a P-glycoprotein substrate; see Soldner, A.; Benet, L. Z.; Mutschler, E.; Christians, U. Active Transport of the Angiotensin-II Antagonist Losartan and its Main Metabolite EXP 3174 Across MDCK-MDR1 and Caco-2 Cell Monolayers. *Br. J. Pharmacol*. **2000**, *129*, 1235−1243.

(10) (a) Senanayake, C. H.; Fredenburgh, L. E.; Reamer, R. A.; Liu, J.; Roberts, F. E.; Humphrey, G.; Thompson, A. S.; Larsen, R. D.; Verhoeven, T. R.; Reider, P. J.; Shinkai, I. New Approach to the Imidazolutidine Moiety of MK-996. *Heterocycles* **1996**, *42*, 821−830. (b) Chakravarty, P. K.; Greenlee, W. J.; Mantlo, N. B.; Patchett, A. A.; Walsh, T. F. Substituted Imidazo-Fused 6-membered Heterocycles as Angiotensin II Antagonists. U. S. Patent 5,332,744, 1994. *Chem. Abstr. 123*, 143911.

(11) Echavarren, A. M.; Stille, J. K. Palladium-Catalyzed Coupling of Aryl Triflates with Organostannanes. *J. Am. Chem. Soc.* **1987**, *109*, 5478−5486..

(12) Marck, G.; Villiger, A.; Buchecker, R. Aryl Couplings with Heterogeneous Palladium Catalysts. *Tetrahedron Lett*. **1994**, *35*, 3277−3280.

(13) Walsh, D. A. The Synthesis of 2-Aminobenzophenones. *Synthesis* **1980**, 677−688.

(14) Tawada, H.; Harcourt, M.; Kawamura, N.; Kajino, M.; Ishikawa, E.; Sugiyama, Y.; Ikeda, H.; Meguro, K. Novel Acyl-CoA: Cholesterol Acyltransferase Inhibitors. Synthesis and Biological Activity of 3-Quinolylurea Derivatives. *J. Med. Chem*. **1994**, *37*, 2079−2084.

(15) Anzini, M.; Cappelli, A.; Vomero, S.; Giorgi, G.; Langer, T.; Hamon, M.; Merahi, N.; Emerit, B. M.; Cagnotto, A.; Skorupska, M.; Mennini, T.; Pinto, J. C. Novel, Potent, and Selective 5-HT_3 Receptor Antagonists Based on the Arylpiperazine Skeleton: Synthesis, Structure, Biological Activity, and Comparative Molecular Field Analysis Studies. *J. Med. Chem*. **1995**, *38*, 2692−2704.

(16) Chakravarty, P. K.; Maccross, M.; Mantlo, N. B.; Walsh, T. F. Preparation and Use of N−Benzylareneimidazole Derivatives as Angiotensin II Antagonists. U. S. Patent 5,128,327, 1992. *Chem. Abstr. 123*, 228187.

(17) Chang, R. S. L.; Siegl, P. K. S.; Clineschmidt, B. W.; Mantlo, N. B.; Chakravarty, P. K.; Greenlee, W. J.; Patchett, A. A.; Lotti, V. J. In vitro Pharmacology of L-158, 809, a New Highly Potent and Selective Angiotensin II Receptor Antagonists. *J. Pharmacol. Exp. Ther*. **1992**, *262*, 133−138.

(18) Naphthalene derivative **4a** was described in a patent application (see Suzuki, K.; Fujiwara, S.; Machii, D.; Ochifuji, N.; Takai, H.; Oono, T.; Furuta, S.; Yamada, K. Preparation of Imidazopyridines and Analogs as Angiotensin II Antagonists. Jpn. Kokai Tokkyo Koho JP 06 92,939, 1994. *Chem. Abstr. 121*, 179581 and Fujiwara, S.; Takai, H.; Mizukami, T.; Myaji, H.; Sato, S.; Oomori, T.; Nukui, E. Preparation of N-[4-(4-Quinolinyl)benzyl]-benzimidazole Derivatives as Immunosuppressants. Jpn. Kokai Tokkyo Koho JP 06,340,658, 1994. *Chem. Abstr. 122*, 239702) and resynthesized in our laboratory as a reference compound for our quinoline derivatives.

(19) Carini, D. J.; Duncia, J. V.; Aldrich, P. E.; Chiu, A. T.; Johnson, A. L.; Pierce, M. E.; Price, W. A.; Santella, J. B., III; Wells, G. J.; Wexler, R. R.; Wong, P. C.; Yoo, S.-E.; Timmermans, P. B. M. W. M. Nonpeptide Angiotensin II Receptor Antagonists: The Discovery of a Series of *N*-(Biphenylmethyl)imidazoles as Potent, Orally Active Antihypertensives. *J. Med. Chem*. **1991**, *34*, 2525−2547.

(20) The different prototropic tautomerism behavior of the heterocyclic amino derivatives with respect to the corresponding hydroxy derivatives has been discussed by Katritzky, A. R. and co-workers (Katritzky, A. R.; Karelson, M.; Harris, P. A. Prototropic Tautomerism of Heteroaromatic Compounds. *Heterocycles*, **1991**, *32*, 329−369). These authors pointed out that 2-aminopyridine exists predominantly in the amino-form, while 2-pyridones exist in the oxo-form.

(21) Kurup, A.; Garg, R.; Carini, D. J.; Hansch, C. Comparative QSAR: Angiotensin II Antagonists. *Chem. Rev*. **2001**, *101*, 2727−2750.

(22) Karelson, M.; Lobanov, V. S.; Katritzky, A. R. Quantum-Chemical Descriptors in QSAR/QSPR Studies. *Chem. Rev*. **1996**, *96*, 1027−1043.

(23) Beukers, M. W.; Kristiansen, K.; Ijzerman, A. P.; Edvardsen, Ø. TinyGRAP Database: a Bioinformatics Tool to Mine G Protein-Coupled Receptor Mutant Data. *Trends Pharmacol. Sci*. **1999**, *20*, 475−477.

(24) Henderson, R.; Baldwin, J.; Ceska, T. H.; Zemlin, F.; Beckmamn, E.; Downing, K. Model of the Structure of Bacteriorhodopsin Based on High-Resolution Electron Cryomicroscopy. *J. Mol. Biol*. **1990**, *213*, 899−919.

(25) Baldwin, J. M. The Probable Arrangement of the Helices in G Protein-Coupled Receptors. *EMBO J*. **1993**, *12*, 1693−1703.

(26) Palczewski, K.; Kumasaka, T.; Hori, T.; Behnke, C. A.; Motoshima, H.; Fox, B. A.; Le Trong, I.; Teller, D. C.; Okada, T.; Stenkamp, R. E.; Yamamoto, M.; Miyano, M. Crystal Structure of Rhodopsin: A G-Protein-Coupled Receptor. *Science*, **2000**, *289*, 739−745

(27) Wilkes, B. C.; Masaro, L.; Schiller, P. W.; Carpenter, K. A. Angiotensin II vs its Type I Antagonists: Conformational Requirements for Receptor Binding Assessed from NMR Spectroscopic and Receptor Docking Experiments. *J. Med. Chem*. **2002**, *45*, 4410−4418.

(28) Robertson, M. J.; Cunoosamy, M. P.; Clark, K. L. Effects of Peptidase Inhibition on Angiotensin Receptor Agonist and Antagonist Potency in Rabbit Isolated Thoracic Aorta. *Br. J. Pharmacol*. **1992**, *106*, 166−172.

(29) Ji, H.; Zheng, W.; Zhang, Y.; Catt, K. J.; Sandberg, K. Genetic Transfer of a Nonpeptide Antagonist Binding Site to a Previously RT Unresponsive Angiotensin Receptor. *Proc. Natl. Acad. Sci. U.S.A*. **1995**, *92*, 9240−9244.

(30) Sheldrick, G. M. SHELXS-97, Rel. 97−2, Program for X-ray data diffraction, Gottingen University, 1997.

(31) Sheldrick, G. M. SHELXL-97, Rel. 97−2, Program for X-ray data diffraction, Gottingen University, 1997.

(32) Dewar, M. J. S.; Zoebisch, E. G.; Healey, E. F.; Stewart, J. J. P. AM1: A New General Purpose Quantum Mechanical Molecular Model. *J. Am. Chem. Soc*. **1985**, *107*, 3902−3909.

(33) Sali, A.; Blundell, T. L. Comparative Protein Modeling by Satisfaction of Spatial Restraints. *J. Mol. Biol*. **1993**, *234*, 779−815.

(34) Thompson, J. D.; Higgins, D. G.; Gibson, T.; Clustal, W. Improving the Sensitivity of Progressive Multiple Sequence Alignment through Sequence Weighting, Position-Specific Gap Penalties and Weight Matrix Choice. *J. Nucleic Acids Res*. **1994**, *22*, 4673−4680.

(35) Quanta98, 1998 Accelrys, San Diego, CA.

(36) Brooks, B. R.; Bruccoleri, R. E.; Olafson, B. D.; States, D. J.; Swaminathan, S.; Karplus, M. CHARMM: a Program for Macromolecular Energy Minimization and Dynamics Calculations. *J. Comput. Chem*. **1983**, *4*, 187−217.

(37) van Gunsteren, W. F.; Berendsen, J. C. Algorithms for Macromolecular Dynamics and Constraint Dynamics. *Mol. Phys*. **1977**, *34*, 1311−1327.

JM031100T